Measurement of the $E \times B$ velocity across the LOC-SOC transition

A. Lebschy[1,2], R. M. McDermott[1], C. Angioni[1], B. Geiger[1], M. Cavedon[1,2], G. D. Conway[1], R. Dux[1], E. Fable[1], T. Happel[1], A. Kappatou[1], A. Medvedeva[1,2,3], T. Pütterich[1], D. Prisiazhniuk[1,2], F. Ryter[1], U. Stroth[1,2], E. Viezzer[1,4] and the ASDEX Upgrade Team[1]

[1] *Max-Planck-Institut für Plasmaphysik, Boltzmannstr. 2, D-85748 Garching, Germany*

[2] *Physik-Department E28, Technische Universität München, D-85748 Garching, Germany,*

[3] *CEA, IRFM, F-13108 Saint-Paul-Lez-Durance, France,*

[4] *Dpt. of Atomic, Molecular and Nuclear Physics, University of Seville, Avda. Reina Mercedes, 41012 Seville, Spain*

Introduction

It was found in the early 80's that there are two different confinement regimes in low density ohmically heated tokamak plasmas, namely the linear ohmic confinement (LOC) and saturated ohmic confinement (SOC) regime. These two regimes are characterized by the energy confinement time (τ_E) that increases linearly with the density of the plasma in LOC and saturates above a certain threshold density defining the SOC regime [1].

This behavior can be seen in figure 1 showing an ohmically heated L-mode discharge at ASDEX Upgrade (AUG). Through a feedback density ramp, the electron density (n_e) is increased in this discharge and the LOC-SOC transition happens at an averaged electron density of roughly $1.6 \cdot 10^{19}\,\mathrm{m}^{-3}$. This figure shows as well a comparison to some scalings: the slope of τ_E agrees very well with the neo-Alcator scaling obtained for LOC. In SOC, there is a very good agreement with the ITER89-P scaling.

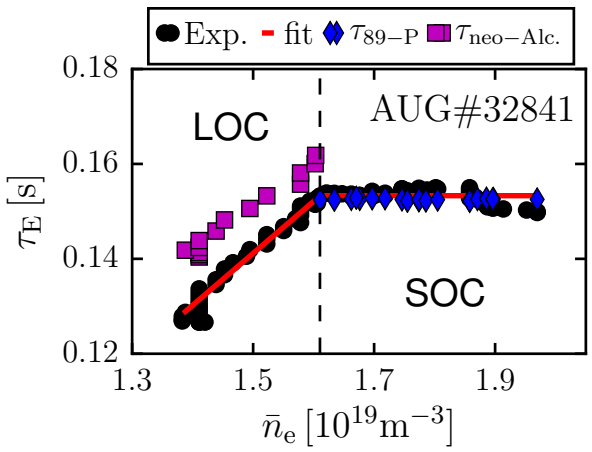

Figure 1: τ_E is calculated from the thermal energies of electrons and ions and shown as a function of the averaged electron density. The measured τ_E values are compared to the neo-Alcator [4] LOC and the ITER89-P [5] SOC scaling.

One hypothesis that has been considered for a long time is that the transition from LOC to SOC regime is due to a change in the dominant turbulence regime from trapped electron mode (TEM) in LOC to ion temperature gradient (ITG) in SOC [2]. The increase in τ_E in the LOC regime is then attributed to the de-trapping of trapped electrons and an improved coupling between electrons and ions. The ions confine the energy better due to their lower temperature gradient and lower thermal diffusivity. In the SOC regime, the thermal diffusivity of electrons and ions become independent of n_e and the energy exhaust is covered by ITG [3].

To date, experimental investigations have not been able to either confirm or refute this picture and the physics of this transition requires, therefore, further assessment. One way to gain additional information on the type of turbulence present in these plasma would be to directly measure the phase velocity (v_{ph}) of the turbulence. v_{ph} is expected to be in the electron diamagnetic direction for TEM and in the ion diamagnetic direction for ITG. A change in the sign of the propagation direction would indicate a change in the turbulence properties.

At AUG multiple reflectometry systems measure the perpendicular velocity $u_{\perp}$ of density fluctuations in the plasma: $u_{\perp} = u_{E\times B} + v_{\mathrm{ph}}$. The phase velocity of the turbulence, however, is expected to be much smaller than $u_{\perp}$ or $u_{E\times B}$; such that a very accurate measurement of both quantities is necessary in order to detect a change of v_{ph}.

Due to an upgrade of the core CXRS systems at AUG it is now possible to have a precise measurement, although it is indirect, of the poloidal rotation (u_{pol}) in the plasma core [6]. This measurement is based on the evaluation of the toroidal rotation (u_{tor}) at two points on the same flux surface. An asymmetry in the toroidal rotation frequency $\omega_{\mathrm{tor}} = u_{\mathrm{tor}}/R$ between low-field side and high-field side indicates the existence of a poloidal flow [7, 8]. This measurement of u_{pol} in the plasma core allows for the evaluation of the radial electric field (E_{r}) from the radial force balance equation for a given ion species α and, therefore, enables the measurement of $u_{E\times B}$ in the plasma core:

$$E_{\mathrm{r}} = \frac{\nabla p_{\alpha}}{e Z_{\alpha} n_{\alpha}} - u_{\mathrm{pol},\alpha} B_{\mathrm{tor}} + u_{\mathrm{tor},\alpha} B_{\mathrm{pol}}. \tag{1}$$

Here, ∇p_{α} denotes the radial pressure gradient, eZ_{α} the charge and n_{α} the density of the species α. B_{pol} and B_{tor} are the poloidal and toroidal magnetic field components determined from the magnetic equilibrium reconstruction. This measurement can be made with an accuracy better than $\pm 1\,\mathrm{km/s}$ in LOC-SOC discharges enabling to resolve phase velocities in the order of $1\,\mathrm{km/s}$.

Reversal of the core intrinsic rotation

In the same parameter range in which LOC-SOC transitions occur, i. e. in low density L-mode plasmas, the core toroidal rotation decreases and changes from the co- to the counter-current direction. This has been observed at Alcator C-Mod [9], AUG [10, 11], TCV [12] and KSTAR [13] and is in-line with AUG Doppler reflectometry measurements across the LOC-SOC transition [14]. This change in u_{tor} could be attributed to a residual stress mechanism that changes sign with the sign of v_{ph} [15]. At AUG, the gradient in the toroidal rotation changes back towards co-current values when the density is increased even further in the SOC regime [11] making his explanation insufficient. The work presented in [11] rather suggests that is the normalized logarithmic electron density gradient ($R/L_{n_{\mathrm{e}}}$) that is leading to the rotation reversal. The observation agrees with the fact that the rotation gradient at around mid-radius determines the core toroidal rotation [10]. As large values of $R/L_{n_{\mathrm{e}}}$ occur only near the boundary between

TEM and ITG turbulence regimes [16], the reversal of the core rotation could be caused by changes of the electron density profiles happening close to the LOC-SOC transition but not by the transition itself [11].

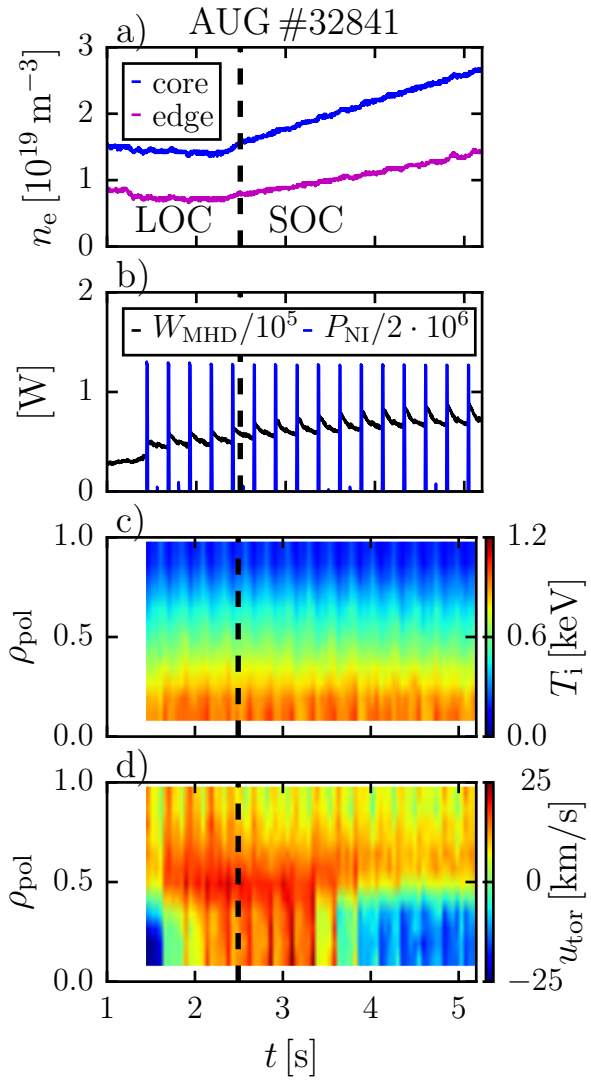

Figure 2: From top to bottom, time evolution of (a) the electron density, (b) the plasma stored energy (W_{MHD}) and the timing of the NBI blips in blue, (c) a contour plot of the ion temperature and (d) the toroidal rotation for a low density L-mode plasma with a density ramp.

Figure 2 shows timetraces of AUG discharge #32841 with a LOC-SOC transition and a reversal of u_{tor}. In order to measure the $E \times B$ velocity, beam blips are injected into the plasma for CXRS measurements with a repetition rate of 4 Hz and a length of 16 ms (see figure 2(b)). In between these blips, there are 5 ms 'conditioning blips' for the neutral beam injection (NBI) source. These short blips discharge the capacitor of the NBI giving the best performance of the NBI source. The timing of the blips is chosen such that W_{MHD} decays fully to its original value before the next blip and that there is no build up of current momentum from the NBI blips. In order to gain information on the CXRS profiles before the beam blip, a back-extrapolation method is used [17]. Thus, the measured rotation is the intrinsic rotation of the plasma.

As shown in figure 2(d), the plasma starts with a counter-current toroidal rotation in the core, i.e. with a negative sign, which could be associated with the fact that the shape of the plasma is not fully developed until 1.5 s. The evolution of the profiles and the shape can influence the toroidal rotation so that it starts in the counter-current direction [18]. The core rotation switches in the co-current direction at 2 s as the electron density is increased and the plasma transitions from the LOC to the SOC regime at 2.5 s and an averaged density of $1.6 \cdot 10^{19}\,m^{-3}$. As the density is increased even further, the rotation profile becomes flat and, subsequently, hollow in the plasma core and transitions from co- to the counter-current direction. It can be clearly seen that there is a delay between the LOC-SOC transition, the change in the core rotation gradient at mid-radius and, finally, the rotation reversal. The ion temperature profile stays almost unchanged throughout the discharge (see figure 2(c)).

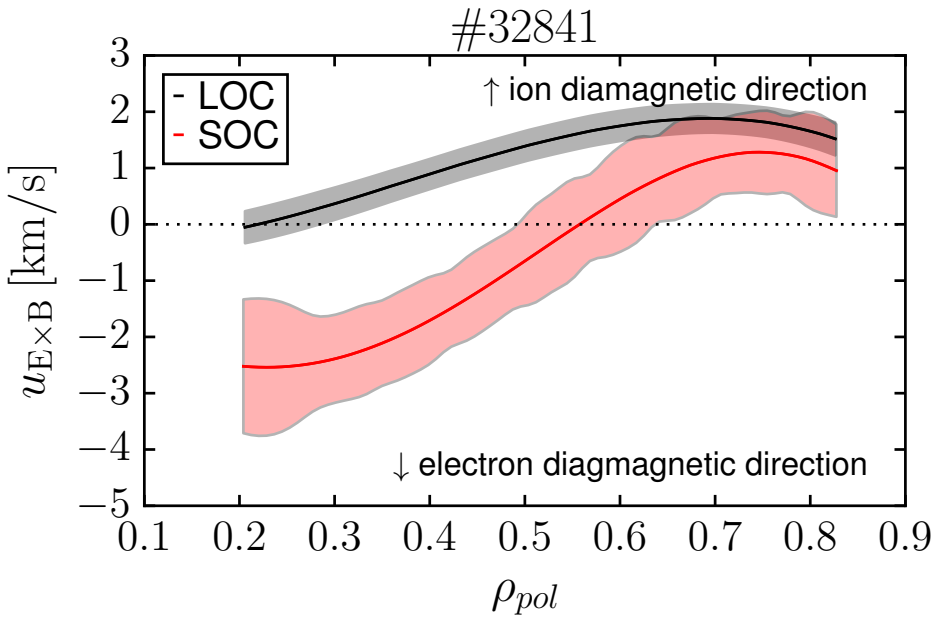

Figure 3: Measured $E \times B$ velocities for one time point in the LOC and one in the SOC regime.

Measurement of the $E \times B$ velocity across the LOC-SOC transition

Using the capabilities of the new diagnostic, the core poloidal rotation has been measured across the LOC-SOC transition as it is shown in figure 3. It can be seen that in LOC, the $E \times B$ velocity is in the ion diamagnetic direction across the whole profile. After the reversal of the core rotation, the $E \times B$ velocity in the SOC regime changes sign to the electron diamagnetic direction at mid-radius. The increase in the error bars between the two time points is associated to the decreased impurity concentration and signal level at higher densities.

From the measurement it seems that the poloidal rotations is smaller in the LOC regime than expected from neoclassical (NC) theory, which is calculated using the code NEOART [19]. The difference of u_{pol} in LOC with respect to NC theory leads to higher $E \times B$ velocities which is consistent with measurements with a newly installed poloidal correlation reflectometry diagnostic [20] and could explain previously observed differences between CXRS and reflectometry measurements [11].

Acknowledgment

This work has been carried out within the framework of the EUROfusion Consortium and has received funding from the Euratom research and training programme 2014-2018 under grant agreement No 633053. The views and opinions expressed herein do not necessarily reflect those of the European Commission.

References

[1] S. Ejima *et. al*, NF **22** (1982) 1672
[2] F. Wagner and U. Stroth, PPCF **35** (1993) 1321
[3] U. Stroth, PPCF **40** (1998) 9-74
[4] R. J. Goldston, PPCF **26** (1984) 87
[5] P. N. Yushmanov *et. al*, NF **30** (1990) 1999
[6] A. Lebschy *et al.*, 42th EPS (2015) P 1.137
[7] C. Chrystal *et al.*, RSI **83** (2012) 10D501
[8] A. Bortolon *et al.*, NF **53** 023002
[9] J. E. Rice *et al.*, PPCF **50** (2008) 124042
[10] C. Angioni *et al.*, PRL **107** (2011) 215003
[11] R. M. McDermott *et al.*, NF **54** (2014) 043009
[12] A. Bortolon *et al.*, PRL **97** (2006) 235003
[13] Y. J. Shi *et al.*, NF **53** (2013) 113031
[14] G. D. Conway *et al.*, NF **46** (2006) S799-S808
[15] Y. Camenen *et al.*, NF **51** (2011) 073039
[16] C. Angioni *et al.*, NF **52** (2012) 114003
[17] R. M. McDermott *et al.*, PPCF **53** (2011) 124013
[18] E. Fable *et al.*, NF **52** (2012) 063017
[19] A. G. Peeters, PoP **7** (2000) 268-275
[20] D. Prisiazhniuk *et al.*, to be submitted to PPCF